

See discussions, stats, and author profiles for this publication at: <https://www.researchgate.net/publication/277554343>

Trends in the Reactivity of the $\text{CpMn}(\text{CO})_2(\eta^2\text{-arene})$ Bond [arene) benzene, toluene, o-xylene, m-xylene, p-xylene, and mesitylene]: An Experimental and Theoretical Investigation

RESEARCH · JUNE 2015

READS

131

1 AUTHOR:



[Khaldoon Al-Obaidi](#)

University of Aberdeen

23 PUBLICATIONS 2 CITATIONS

SEE PROFILE

Trends in the Reactivity of the $\text{CpMn(CO)}_2(\eta^2\text{-arene})$ Bond [arene = benzene, toluene, *o*-xylene, *m*-xylene, *p*-xylene, and mesitylene]: An Experimental and Theoretical Investigation

Ashfaq A. Bengali,^{*,†} Wai Yip Fan,[‡] and Khaldoon T. Abdulrazak[†]

Department of Chemistry, Texas A&M University Qatar, P.O. Box 23874, Doha, Qatar, and Department of Chemistry, National University of Singapore, 3 Science Drive, Singapore 117543

Received December 15, 2008

The displacement of η^2 -coordinated arenes [arenes = benzene, toluene, *o*-xylene, *m*-xylene, *p*-xylene, and mesitylene] from the photolytically generated $\text{CpMn(CO)}_2(\eta^2\text{-arene})$ complex by pyridine was studied. The substitution reaction proceeds by a dissociative mechanism, and the relative rates of displacement provide information about the interplay between electronic and steric factors in determining the overall stability of the $\text{Mn}-(\eta^2\text{-arene})$ bond. The regioselectivity of metal binding to the arene ligand was determined by examining the observed trends in the relative displacement rates for the xylenes. Theoretical modeling of the $\text{Mn}-(\eta^2\text{-arene})$ complexes lends support for the experimental analysis. Interestingly, unlike the other arenes, DFT (density functional theory) calculations suggest that mesitylene is bound to the Mn center by an arene C–H bond rather than by a C=C edge of the aromatic system.

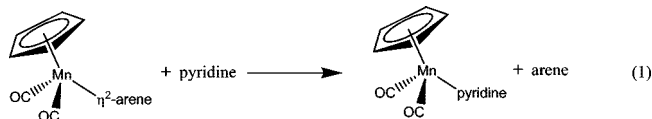
Introduction

Aromatic ligands such as benzene can bind to a transition metal center in several different ways. The most common coordination mode is an η^6 interaction in which the π cloud of the organic ligand interacts with acceptor orbitals on the metal center (e.g., $(\eta^6\text{-C}_6\text{H}_6)\text{Cr(CO)}_3$).¹ In recent years, several complexes have been isolated in which the arene is bound to the metal in an η^2 (dihapto) fashion where the metal center interacts with the π electron density via a C=C edge of the aromatic system.² In addition to examples of such stable systems, weakly bound metal– η^2 aromatic complexes have also been detected and are often invoked as intermediates in the activation of arene C–H bonds.^{3,4} Given the relevance of η^2 -coordinated arene complexes in a number of organic transformations, it is important to investigate the reactivity of such complexes and to understand the factors that influence their stability.

Recently, we studied the formation and subsequent displacement of η^2 -coordinated benzene and substituted benzenes from the $(\eta^6\text{-C}_6\text{H}_5\text{R})\text{Cr(CO)}_2(\eta^2\text{-C}_6\text{H}_5\text{R})$ complexes [R = H, CH₃, CF₃].^{5a} It was found that the stability of the dihapto bond was strengthened when the flow of electrons from ligand to metal was enhanced by either decreasing electron density on the metal

or increasing it on the arene. For example, trifluoromethylbenzene was bound weaker to the Cr center than toluene, presumably due to the electron-withdrawing effects of the CF₃ substituent. Thus, arene \rightarrow metal σ donation was thought to make an important contribution to the overall stability of the $\text{Cr}-(\eta^2\text{-arene})$ interaction.

On the basis of these results, we were interested in systematically increasing the number of CH₃ groups on the arene ring and studying the influence of changing both the electronic and steric properties of the arene ligand upon the reactivity of the resulting metal–(η^2 -arene) bond. Addition of CH₃ groups to the arene ligand is expected to enhance arene \rightarrow metal σ donation, resulting in a more stable interaction. However, addition of these groups also adds to steric crowding, making it more difficult for the arene to approach the metal at an optimum bonding distance. It is therefore of interest to probe the counteracting electronic and steric influences and determine if there is a crossover point at which one of these factors overwhelms the other. Thus, we report in this paper a kinetic study in which the rate of displacement of weakly coordinated η^2 arenes [arenes = benzene, toluene, *o*-xylene, *m*-xylene, *p*-xylene, and mesitylene] from the $\text{CpMn(CO)}_2(\eta^2\text{-arene})$ [Cp = $\eta^5\text{-C}_5\text{H}_5$] complex by pyridine was studied using time-resolved infrared spectroscopy (reaction 1).



The trends in the reactivity of these complexes provide information about the interplay between electronic and steric influences in determining the overall stability of the metal–(η^2 -arene) bond. In conjunction with density functional (DFT) studies, the experimental results also allow us to ascertain the preferred orientation of metal binding to the C=C edge of the aromatic system relative to the CH₃ substituents.

* Corresponding author. E-mail: ashfaq.bengali@qatar.tamu.edu.

[†] Texas A&M University Qatar.

[‡] National University of Singapore.

(1) Kündig, E. P. *Transition Metal Arene π Complexes in Organic Synthesis and Catalysis*; Springer-Verlag: Berlin, 2004.

(2) (a) Keane, J. M.; Harman, W. D. *Organometallics* **2005**, *24*, 1786. (b) Harman, W. D. *Chem. Rev.* **1997**, *97*, 1953.

(3) (a) Bengali, A. A.; Grunbeck, A. R. *Organometallics* **2005**, *24*, 5919.

(b) Bengali, A. A.; Leicht, A. *Organometallics* **2001**, *20*, 1345. (c) Zhang, S.; Dobson, G. R.; Zang, V.; Bajaj, H. C.; van Eldik, R. *Inorg. Chem.* **1990**, *29*, 3477. (d) Wells, J. R.; House, P. G.; Weitz, E. *J. Phys. Chem.* **1994**, *98*, 8343.

(4) (a) Belt, S. T.; Dong, L.; Duckett, S. B.; Jones, W. D.; Partridge, M. G.; Perutz, R. N. *Chem. Commun.* **1991**, 266. (b) Jones, W. D. *Acc. Chem. Res.* **2003**, *36*, 140. (c) Norris, C. M.; Reinartz, S.; White, P. S.; Templeton, J. L. *Organometallics* **2002**, *22*, 5649. (d) Peterson, T. H.; Golden, T.; Bergman, R. G. *J. Am. Chem. Soc.* **2001**, *123*, 455.

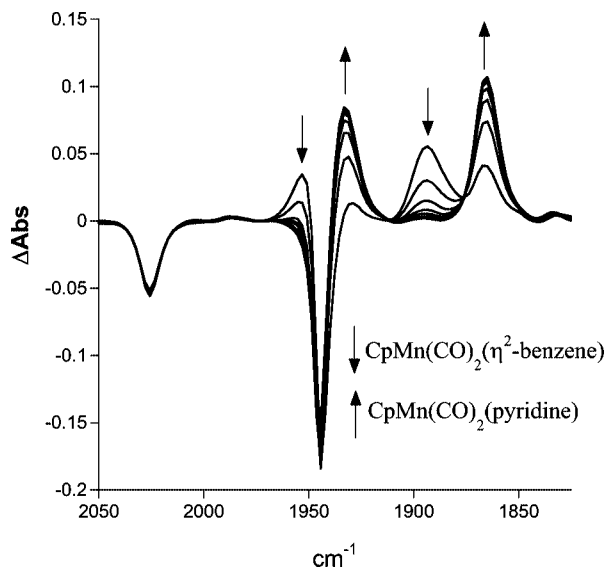


Figure 1. Difference step-scan FTIR spectra obtained upon photolysis of a cyclohexane solution of CpMn(CO)_3 with 1.12 M benzene and 0.031 M pyridine at 296 K. The spectra shown were obtained at 250 μs intervals.

Experimental and Theoretical Details

All kinetic experiments were conducted using a Bruker Vertex 80 FTIR with step-scan capabilities. Sample photolysis was performed using the third harmonic (355 nm) of a Continuum Surelite I-10 Nd:YAG laser operating at 1 Hz. A syringe pump was used to flow solution through a temperature-controlled 0.5 mm path length IR cell with CaF_2 windows (Harrick Scientific) to ensure that a fresh solution was photolyzed with every shot of the laser. The temperature was monitored by a thermocouple located close to the photolysis solution and maintained by a water circulator to within ± 0.1 $^\circ\text{C}$. All spectra were obtained at 8 cm^{-1} resolution.

The photolysis solution contained ~ 4 mM CpMn(CO)_3 in cyclohexane solvent and was 1.12 M in the appropriate arene. Varying amounts of pyridine were added to this solution as the displacing ligand. All kinetic runs were conducted under pseudo-first-order conditions in which the concentration of the incoming ligand was at least 10 times greater than that of the reactant complexes. Observed rate constants (k_{obs}) were obtained from single-exponential fits to the absorbance versus time dependence of the reactant and product complexes. The errors in the reported rate constants were obtained from linear fits to the k_{obs} versus [pyridine] data. All chemicals used were anhydrous grade and of $>97\%$ purity (Alfa Aesar). The CpMn(CO)_3 complex (Strem) was used as received.

The structure, stabilities, and vibrational frequencies of the $\text{CpMn(CO)}_2(\eta^2\text{-arene})$ complexes were studied using the Gaussian 03 program employing the B3LYP functional.⁵ The transition metal, C, H, and O atoms were described by the 6-31G* basis set.

Results and Discussion

As shown in Figure 1, photolysis of a cyclohexane solution of CpMn(CO)_3 in the presence of the appropriate arene and pyridine results in the generation of two dicarbonyl complexes absorbing at ~ 1890 and 1955 cm^{-1} and 1865 and 1932 cm^{-1} . By analogy with the previously observed $\text{CpMn(CO)}_2(\eta^2\text{-toluene})$ complex,⁶ the higher energy bands are assigned to the $\text{CpMn(CO)}_2(\eta^2\text{-arene})$

Table 1. Experimental and Calculated Values of ν_{CO} for the $\text{CpMn(CO)}_2(\eta^2\text{-arene})$ Complexes

arene	ν_{CO} (cm^{-1}) [experimental]	ν_{CO} (cm^{-1}) [calculated] ^a
benzene	1893/1955	1888/1932
toluene	1891/1953	1884/1929
<i>o</i> -xylene	1888/1951	1880/1926
<i>m</i> -xylene	1890/1952	1882/1926
<i>p</i> -xylene	1891/1950	1879/1924
mesitylene	1889/1958	1878/1924

^a B3LYP/6-31G* scaled by a factor of 0.94.

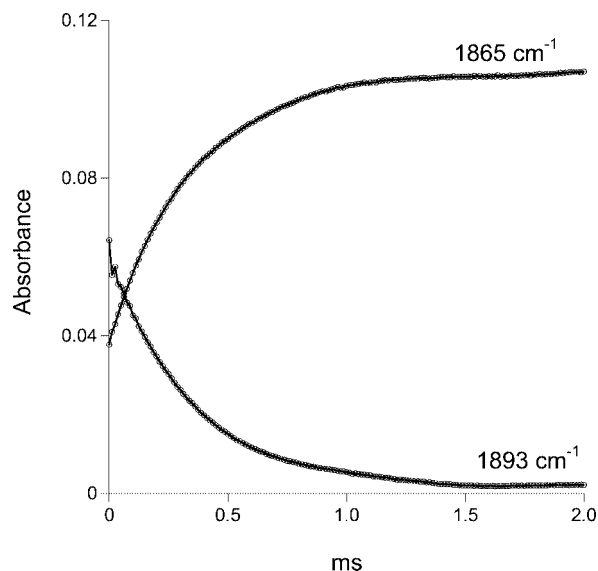


Figure 2. Time-resolved infrared traces following photolysis of a cyclohexane solution of CpMn(CO)_3 containing 1.12 M benzene and 0.031 M pyridine at 296 K. Growth of the $\text{CpMn(CO)}_2(\text{pyridine})$ complex is monitored at 1865 cm^{-1} , while the decay of $\text{CpMn(CO)}_2(\eta^2\text{-benzene})$ is observed at 1893 cm^{-1} .

complex. As noted earlier, there is ample evidence for the formation of both isolable and weakly bound metal-(η^2 -arene) complexes in the literature. The CO stretching frequencies for all the complexes studied are presented in Table 1.

The bands at 1865 and 1932 cm^{-1} are assigned to the previously observed $\text{CpMn(CO)}_2(\text{pyridine})$.⁷ Since the photolysis was carried out in cyclohexane (CyH) solvent, the previously observed $\text{CpMn(CO)}_2(\text{CyH})$ complex is undoubtedly formed immediately upon photolysis.^{8a} However, using the published rate constants and under the experimental conditions used, the conversion of this species to the $\text{CpMn(CO)}_2(\eta^2\text{-arene})$ and $\text{CpMn(CO)}_2(\text{pyridine})$ complexes is estimated to occur within $3\text{--}4$ μs , a time scale considerably shorter than that of the present study. Consequently, the $\text{CpMn(CO)}_2(\text{CyH})$ complex was not observed in experiments conducted in the presence of arene and pyridine.

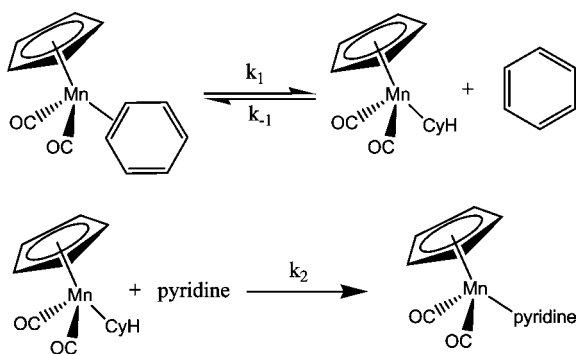
As shown in Figure 2, the $\text{CpMn(CO)}_2(\eta^2\text{-arene})$ complex undergoes a first-order exponential decay, and the $\text{CpMn(CO)}_2(\text{pyridine})$ complex grows at the same rate. In the case of the $\text{CpMn(CO)}_2(\eta^2\text{-toluene})$ complex, the displacement reaction was previously shown to follow a dissociative mechanism.⁶ We therefore assume a similar substitution mechanism is operative for all the arenes studied in the present investigation (Scheme 1). The $\text{CpMn(CO)}_2(\text{CyH})$ complex is the most likely intermediate in this reaction since it has been observed on the microsecond time scale.^{8a} Previous studies have also demonstrated that the displacement of either CyH or heptane from

(5) (a) Frisch, M. J.; et al. *Gaussian 03, Revisions B. and B.05*; Gaussian, Inc.: Wallingford, CT, 2004. (b) Becke, A. D. *J. Phys. Chem.* **1993**, *98*, 5648. (c) Lee, C.; Yang, W.; Parr, R. G. *Phys. Rev. B* **1988**, *37*, 785.

(6) Bengali, A. A. *Organometallics* **2000**, *19*, 4000.

(7) Giordano, P. J.; Wrighton, M. S. *Inorg. Chem.* **1977**, *16*, 160.

Scheme 1



the Mn center proceeds by an interchange pathway.⁸ The above mechanism is therefore consistent with these studies since it assumes that the substitution of CyH by either arene (k_{-1}) or pyridine (k_2) proceeds through a single transition state. Applying the steady state assumption to the intermediate $\text{CpMn}(\text{CO})_2(\text{CyH})$ complex, the dependence of k_{obs} on arene and pyridine concentration is as follows (eq 1):

$$k_{\text{obs}} = \frac{k_1 k_2 [\text{pyridine}]}{k_{-1} [\text{arene}] + k_2 [\text{pyridine}]} \quad (1)$$

Under the experimental conditions of $[\text{pyridine}] \ll [\text{arene}]$,

$$k_{\text{obs}} = \frac{K k_2 [\text{pyridine}]}{[\text{arene}]} \left[K = \frac{k_1}{k_{-1}} \right] \quad (2)$$

To lend support for the dissociative mechanism, the effect of varying the arene concentration upon k_{obs} was studied. For all the arenes studied at 296 K, k_{obs} varies inversely with $[\text{arene}]$. For example, under conditions where $[\text{pyridine}] \ll [\text{benzene}]$, k_{obs} decreases from 5500 s^{-1} to 1900 s^{-1} when $[\text{benzene}]$ is increased from 0.35 to 1.12 M. This inverse dependence of k_{obs} on $[\text{arene}]$ is consistent with a dissociative mechanism for the displacement of the η^2 -bound arene by pyridine (eq 2). While in principle it would be possible to observe saturation of k_{obs} at high $[\text{pyridine}]$, experiments were conducted with $[\text{pyridine}] \ll [\text{arene}]$ so that the reaction rates for all the arenes could be studied under similar conditions. The higher concentrations of $[\text{pyridine}]$ required to achieve saturation of k_{obs} would result in very fast reaction rates for some of the arenes (e.g., mesitylene), which could not be measured reliably. Furthermore, a high concentration of pyridine would also mean that a larger fraction of the initially formed $\text{CpMn}(\text{CO})_2(\text{CyH})$ complex would be trapped as $\text{CpMn}(\text{CO})_2(\text{pyridine})$, resulting in an unacceptable loss of signal for the $\text{CpMn}(\text{CO})_2(\eta^2\text{-arene})$ complex.

Under the experimental conditions, and consistent with the mechanism shown in Scheme 1, k_{obs} exhibits a linear dependence on $[\text{pyridine}]/[\text{arene}]$. These plots have small nonzero intercepts, which are consistent with side reactions such as dimerization of the $\text{CpMn}(\text{CO})_2(\text{solvent})$ complex in the absence of L and reaction with residual water.^{8,9} Since the intercepts have values less than 1% of the slopes, they were not considered to be of significance in the interpretation of the data. Thus, the background decay rates were subtracted from the k_{obs} values, and the resulting plots are shown in Figure 3. The slopes of these plots yield Kk_2 for the arenes studied. Since, k_2 is expected to

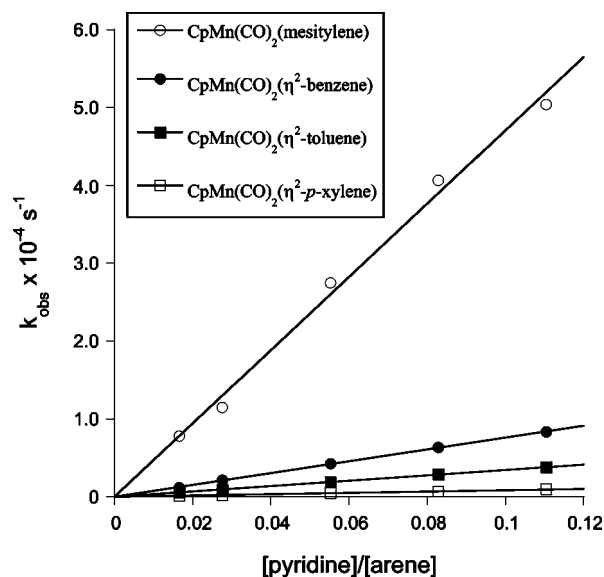


Figure 3. Plot of k_{obs} versus $[\text{pyridine}]/[\text{arene}]$ for reaction 1 at 296 K. The solid lines represent linear fits to the data. The slopes yield values for Kk_2 according to eq 2.

Table 2. Kinetic Parameters Obtained at 296 K from the Slopes of the k_{obs} vs $[\text{Pyridine}]/[\text{Arene}]$ Plots Shown in Figures 3 and 6^a

arene	$Kk_2 \times 10^{-3} (\text{s}^{-1})$	$K_{\text{arene}}/K_{\text{benzene}}$
mesitylene	470.6 ± 23.3	6.20
trifluoromethylbenzene	141.8 ± 2.0	1.87
benzene	75.9 ± 1.1	1.00
toluene	34.3 ± 0.6	0.45
o-xylene	30.9 ± 0.9	0.41
m-xylene	26.7 ± 1.3	0.35
p-xylene	8.5 ± 0.4	0.11

^a The ratio $K_{\text{arene}}/K_{\text{benzene}}$ reflects the relative stabilities of the $\text{CpMn}(\text{CO})_2(\eta^2\text{-arene})$ and $\text{CpMn}(\text{CO})_2(\eta^2\text{-benzene})$ interactions, with a lower value suggestive of a more stable $\text{Mn}-(\eta^2\text{-arene})$ bond.

be constant in all cases, the ratio of the slopes of each plot relative to that of benzene (i.e., $K_{\text{arene}}/K_{\text{benzene}}$) yields information about the relative stabilities of the $\text{CpMn}(\text{CO})_2(\eta^2\text{-arene})$ complexes. In this regard it is assumed that these differences in reactivity are primarily due to variations in the bond dissociation enthalpies of the $\text{Mn}-(\eta^2\text{-arene})$ bonds and that therefore a $K_{\text{arene}}/K_{\text{benzene}}$ ratio of less than 1 refers to a more stable $\text{Mn}-(\eta^2\text{-arene})$ interaction relative to $\text{Mn}-(\eta^2\text{-benzene})$. This assumption is consistent with the results of the DFT study discussed later. The relevant kinetic parameters are presented in Table 2.

The results indicate that as the degree of methyl substitution increases from benzene to the xylenes, the $K_{\text{arene}}/K_{\text{benzene}}$ ratios decrease, suggesting that the stability of the $\text{Mn}-(\eta^2\text{-arene})$ bond increases relative to benzene. This result is perhaps not surprising if inductive effects are taken into consideration. Thus, increasing the number of methyl groups should lead to a progressively more electron-rich arene, resulting in greater arene \rightarrow metal σ donation. Consequently, a more stable bond is expected, resulting in a slower rate of η^2 -arene displacement by pyridine.

To verify that arene \rightarrow metal σ donation makes an important contribution to the overall stability of the $\text{Mn}-(\eta^2\text{-arene})$ bond, the displacement of trifluoromethylbenzene from the Mn center by pyridine was also studied. As shown in Figure 4, the displacement rate for $\text{C}_6\text{H}_5\text{CF}_3$ is almost 5 times faster than that of $\text{C}_6\text{H}_5\text{CH}_3$, consistent with a weakening of the $\text{Mn}-(\eta^2\text{-arene})$ interaction in the case of the electron-deficient arene. A similar

(8) (a) Lugovskoy, S.; Lin, J.; Schultz, R. H. *Dalton Trans.* **2003**, 3103. (b) Grills, D. C.; Sun, X. Z.; Childs, G. L.; George, M. W. *J. Phys. Chem. A* **2000**, *104*, 4300.

(9) Creaven, B. S.; Dixon, A. J.; Kelly, J. M.; Long, C.; Poliakoff, M. *Organometallics* **1987**, *6*, 2600.

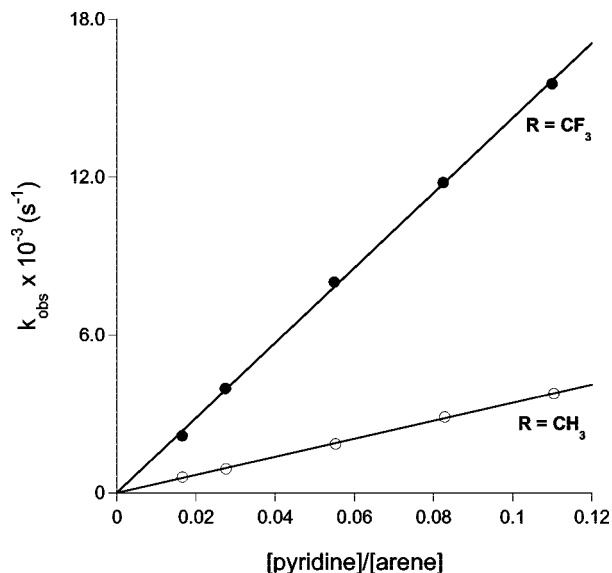


Figure 4. Plot of k_{obs} versus $[\text{pyridine}]/[\text{arene}]$ for the displacement of the η^2 -bound arene from $\text{CpMn}(\text{CO})_2(\eta^2\text{-C}_6\text{H}_5\text{R})$ [$\text{R} = \text{CH}_3, \text{CF}_3$] by pyridine at 296 K.

effect has been observed previously in the case of the $(\eta^6\text{-C}_6\text{H}_5\text{R})\text{Cr}(\text{CO})_2(\eta^2\text{-C}_6\text{H}_5\text{R})$ complexes.^{3a} Thus, it may be concluded that increasing the number of methyl groups from benzene to the xylenes results in a more stable metal–(η^2 -arene) bond primarily due to inductive effects.

The trend in the stabilities of these complexes is markedly different from that observed for the more π basic metals. For the strong metal π bases (W, Mo, Os, Rh, etc.), which disrupt the aromaticity of the bound ligands, the metal–(η^2 -arene) interaction is weakened as the degree of methyl substitution is systematically increased on the arene ring. For example, in contrast to the $\text{CpMn}(\text{CO})_2(\eta^2\text{-arene})$ system, addition of methyl groups to the benzene ring in $[\text{Os}(\text{NH}_3)(\eta^2\text{-C}_6\text{H}_6)]^{2+}$ results in an increase in the substitution rate of the arene ligand.¹⁰ Furthermore, addition of the electron-withdrawing CF_3 group to the benzene ring has an opposite effect and results in a more stable metal–(η^2 -arene) interaction.¹¹ This difference in reactivity is due to the increased importance of π back-bonding relative to σ bonding in the case of the electron-rich metal centers. While increasing the electron density on the arene ligand strengthens the σ interaction, it reduces the degree of metal \rightarrow arene π back-bonding, leading to a weaker bond. For the less electron-rich $\text{CpMn}(\text{CO})_2(\eta^2\text{-arene})$ and $\text{BzCr}(\text{CO})_2(\eta^2\text{-arene})$ complexes, the opposite effect is observed, since $\text{M} \rightarrow \text{L}$ σ bonding is the dominant interaction.

Interestingly, as shown in Figure 5, addition of a third methyl group reverses the trend and results in a significantly higher rate of displacement of mesitylene suggestive of a considerably weaker interaction between the Mn center and mesitylene. In this case, symmetric distribution of the methyl groups on the aromatic ring necessitates the presence of a methyl substituent on one of the carbon atoms coordinated to the metal center. It is reasonable to assume that the increased steric interaction prevents the arene from approaching the metal center at an optimum distance for bonding and results in a weaker interaction relative to the other arenes studied. The data therefore suggest

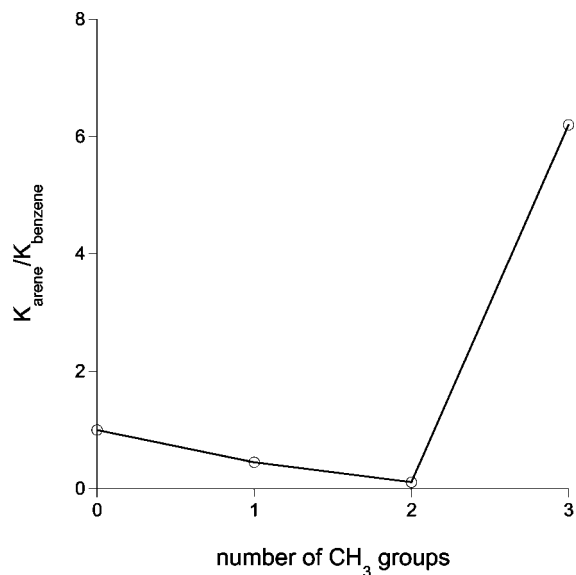


Figure 5. Plot of $K_{\text{arene}}/K_{\text{benzene}}$ versus the number of CH_3 substituents on the η^2 -coordinated arene (arene = benzene, toluene, *p*-xylene, mesitylene) in $\text{CpMn}(\text{CO})_2(\eta^2\text{-arene})$.

that while systematic addition of methyl groups to the η^2 -bound arene results in a progressively more stable interaction due to inductive effects, the crossover point when steric influences begin to dominate electronic factors occurs upon the addition of a third methyl group in the case of mesitylene.

Given the similarity in the positions of the CO bands in $\text{CpMn}(\text{CO})_2(\text{CyH})$ [1891 and 1958 cm^{-1}]^{8a} and $\text{CpMn}(\text{CO})_2(\text{mesitylene})$ [1889 and 1958 cm^{-1}], there is a possibility that steric hindrance in the case of mesitylene prevents binding of this arene ligand to the Mn center altogether and that in fact only the $\text{CpMn}(\text{CO})_2(\text{CyH})$ complex is observed. However, under identical conditions of temperature and $[\text{pyridine}]$, the transient signal at $\sim 1890\text{ cm}^{-1}$ formed upon photolysis of $\text{CpMn}(\text{CO})_3$ in CyH disappears almost 10 times faster in the absence of mesitylene than in its presence. Thus, we conclude that under the present experimental conditions, mesitylene does bind to the Mn center and that this interaction is stronger than that between Mn and cyclohexane. However, theoretical studies discussed later demonstrate that the nature of Mn–mesitylene interaction is different from that of the other arenes.

The differences in the displacement rates of the *o*-, *m*-, and *p*-xylenes yield interesting insight into the preferred binding orientation of the metal relative to the CH_3 substituents. As shown in Figure 6, the displacement rate constants of xylenes from the Mn center, and therefore $K_{\text{arene}}/K_{\text{benzene}}$, decrease in the order *o*-xylene > *m*-xylene > *p*-xylene. Assuming that placement of the CH_3 group on one of the coordinated carbon atoms is unfavorable due to increased steric interaction (as in the case of mesitylene), there is only one possible binding orientation in the case of *p*-xylene. In this instance, both CH_3 groups must be adjacent to the carbon atoms bound to the Mn center. Since the data demonstrate that this is also the most stable interaction, it may be concluded that the CH_3 groups prefer to be as close to the η^2 binding site as possible without being situated on the carbon atoms bound to the metal. Thus, in the case of toluene and *o*-, *m*-, and *p*-xylene, the structures in Figure 7 are expected to be the most stable.

Interestingly, the above regioselectivity of coordination is the same as that calculated for the η^2 binding of fluoroarenes,

(10) Harman, W. D.; Sekine, M.; Taube, H. *J. Am. Chem. Soc.* **1988**, *110*, 5725.

(11) Welch, K. D.; Harrison, D. P.; Lis, E. C.; Liu, W.; Saloman, R. J.; Harman, W. D. *Organometallics* **2007**, *26*, 2791.

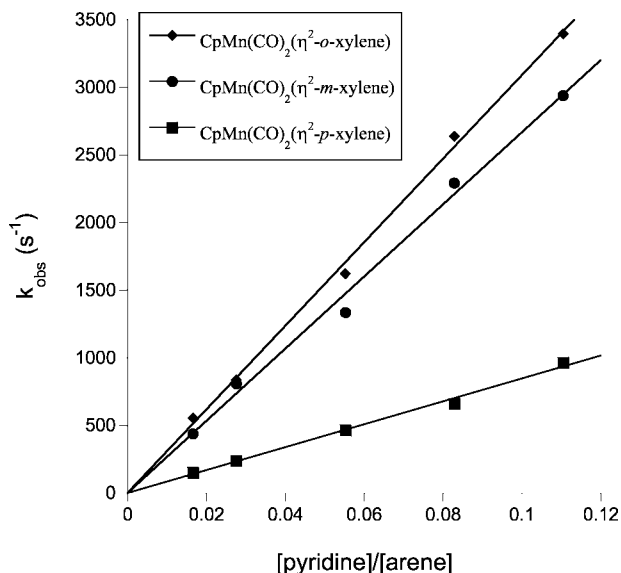


Figure 6. Plot of k_{obs} versus $[\text{pyridine}]/[\text{arene}]$ for the displacement of the η^2 -coordinated arene from $\text{CpMn(CO)}_2(\eta^2\text{-arene})$ by pyridine at 296 K.

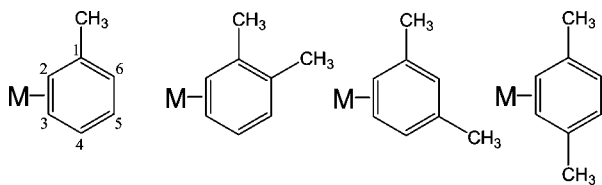


Figure 7. Preferred coordination sites for η^2 binding of arenes to the CpMn(CO)_2 [M] fragment.

$\text{C}_6\text{H}_n\text{F}_{6-n}$ ($n = 5, 4, 3$), to the CpRe(CO)_2 fragment.¹² Thus, in the case of $\text{C}_6\text{H}_5\text{F}$ and *o*-, *m*-, *p*- $\text{C}_6\text{H}_4\text{F}_2$, the most stable metal binding position was calculated to be the same as that shown in Figure 7 for the analogous methyl-substituted benzenes. The calculations suggested that a slight localization of electron density due to the presence of the F atom in the free arene resulted in some bonds having greater π character and hence stronger donor characteristics than others. For example, in the case of $\text{C}_6\text{H}_5\text{F}$, natural bond order (NBO) analysis suggested the double-bond character between C(2) and C(3) was the highest due to a high population in the π and low population in the π^* orbitals of the C=C bond. Consequently, donation of π electron density is more efficient from the C(2)=C(3) site, resulting in a more stable interaction with the metal. A similar situation was found for the difluoroarenes, and in addition, the preferred orientation of the metal center was thought to be dictated by the degree to which π conjugation between F and the arene ring could be retained upon binding. Thus, metal binding to a $\text{HC}=\text{CH}$ bond was preferred over an interaction with a $\text{HC}=\text{CF}$ bond. While conjugation is not possible in the present case, hyperconjugation between the CH_3 group and the π ring system would result in the same regioselectivity of metal binding as that calculated in the case of the fluoroarenes, although the difference in stability between the various regioisomers would be less.

DFT Studies. To lend support to the analysis presented above, the complexes studied experimentally were modeled using density functional theory implemented by Gaussian 03.

Table 3. Binding Energies of Arenes to the CpMn(CO)_2 Fragment^a

arene	binding energy (kJ/mol)
mesitylene	−38.4
benzene	−46.2
toluene	−50.5
<i>o</i> -xylene	−50.6
<i>m</i> -xylene	−52.9
<i>p</i> -xylene	−54.3

^a The energies refer to the structures shown in Figure 7, which were calculated to be the most stable regioisomer.

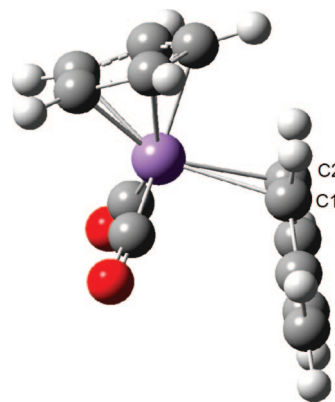


Figure 8. Calculated structure of the $\text{CpMn(CO)}_2(\eta^2\text{-benzene})$ complex at the B3LYP/6-31G* level of theory. Bond distance (C1–C2) = 1.41 Å, and distance from Mn atom to the center of the coordinated C1–C2 bond = 2.35 Å.

The calculated position of the CO stretching bands and the binding energies of the $\text{CpMn(CO)}_2(\eta^2\text{-arene})$ complexes are presented in Tables 1 and 3, respectively. The experimental CO stretching frequencies are in agreement with the calculated and scaled values. The calculated binding energy of 50.5 kJ/mol for the $\text{CpMn(CO)}_2(\eta^2\text{-toluene})$ complex is also in reasonable agreement with the previously determined experimental value of 59.4 kJ/mol.⁶ The concurrence between the experimental and theoretical values suggests that the B3LYP/6-31G* level of theory utilized in this study is adequate for modeling the Mn–(η^2 -arene) complexes. The geometry of the $\text{CpMn(CO)}_2(\eta^2\text{-benzene})$ complex is shown in Figure 8. The minimal perturbation of the ring geometry is in marked contrast to the severe distortions observed upon binding to stronger metal π bases, in which case the ring is completely dearomatized.¹³

Consistent with the experimental data, the calculated binding energies of the complexes exhibit the same trend in stabilities as that deduced from the variation in the displacement rate constants. Thus, the binding energies increase from benzene to the xylenes, and the Mn–mesitylene bond energy is calculated to be significantly weaker than that of the other complexes. The calculated length of the Mn–(η^2 -arene) bond (measured from the metal to the center of the coordinated C=C bond) is also correlated with the strength of the Mn– η^2 interaction. This bond lengthens from 2.29 Å in Mn–(η^2 -*p*-xylene) to 2.35 Å in the relatively weakly bound Mn–(η^2 -benzene) complex. The C=C bond length of the η^2 -coordinated edge of the aromatic ring is slightly longer than the uncoordinated C=C bonds of the aromatic system, providing evidence of some degree of π back-bonding between the metal center and the arene ligand.

Interestingly, the structure of the Mn–mesitylene complex is unlike that of the other molecules studied. As shown in Figure

(12) Clot, E.; Oelckers, B.; Klahn, A. H.; Eisenstein, O.; Perutz, R. N. *Dalton Trans.* **2003**, 4065.

(13) Graham, P. M.; Meiere, S. H.; Sabat, M.; Harman, W. D. *Organometallics* **2003**, *22*, 4364.

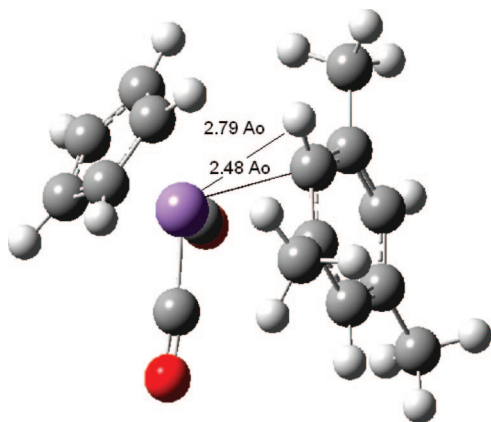


Figure 9. Calculated structure of the $\text{CpMn(CO)}_2(\text{mesitylene})$ complex at the B3LYP/6-31G* level of theory. Note that unlike the structure of the $\text{CpMn(CO)}_2(\eta^2\text{-benzene})$ complex shown in Figure 8, mesitylene binds to the metal center through a C–H rather than a η^2 interaction.

9, the mesitylene solvent is calculated to be bound to the Mn center by an arene C–H bond rather than by a C=C edge of the aromatic system. This difference in binding is most likely behind the large difference in displacement rates between the Mn–mesitylene and the other Mn–(η^2 -arene) complexes studied. In the case of mesitylene, all binding positions result in the close proximity of the CH_3 group to the Mn center. Consequently, the anomalous binding mode of mesitylene is likely due to steric factors, although electronic factors cannot be ruled out. For example, the binding strength of CpRe(CO)_2 to 1,3,5-trifluorobenzene was calculated to be significantly less than to the other trifluoroarenes due to a loss of resonance energy that occurs upon binding of the metal to a $\text{CH}=\text{CF}$ as opposed to a $\text{HC}=\text{CH}$ bond.¹² A similar loss of resonance energy may occur if there is some degree of hyperconjugation between the CH_3 group and the arene ring, resulting in reduced stability when the arene binds through a $\text{HC}=\text{C}(\text{CH}_3)$ bond. The calculations predict a relatively stronger binding of mesitylene to the Mn center through the arene sp^2 C–H bond compared to the interaction between the metal and the aliphatic sp^3 C–H bond in cyclohexane.¹⁴

In cases where there is more than one possible orientation of the metal center relative to the CH_3 groups, i.e., toluene and *o*-xylene, the most stable calculated geometry is one that places the methyl groups as close to the Mn center as possible without situating them on carbon atoms directly bonded to the metal (Figure 7). However, given the small energetic differences between the various regioisomers (calculated to be <3 kJ/mol), it is likely that the kinetic experiments measure an average reactivity of the isomers. Interestingly, for the asymmetric arenes, toluene, *o*-xylene, and *m*-xylene, the coordinated C=C

bond is not oriented symmetrically about the metal. The ring is tilted in the sense that one edge of the C=C bond is pointed in toward the metal center, resulting in slightly unequal Mn–C1 and Mn–C2 bond distances. Presumably, this geometry is adopted due to steric factors.

Conclusions

The displacement of several η^2 -coordinated arenes from the $\text{CpMn(CO)}_2(\eta^2\text{-arene})$ complexes by pyridine was studied. The substitution rate constants decrease in the order benzene $>$ toluene $>$ xylene. These results in conjunction with DFT calculations suggest that addition of CH_3 groups to the benzene ring results in a more stable metal–(η^2 -arene) interaction due to enhanced arene \rightarrow metal σ bonding. The opposite trend is observed in the case of electron-rich metal centers, where metal \rightarrow arene π back-bonding plays a more significant role in the binding interaction.

Steric considerations overwhelm electronic factors in determining the overall stability of the metal–(η^2 -arene) bond upon addition of a third CH_3 group in the case of mesitylene, which results in a significant increase in the displacement rate constant. The results indicate that the metal center prefers binding to the unsubstituted $\text{HC}=\text{CH}$ bond of the arene ligand. The variation of the displacement rate constants in the case of the xylenes (*o*-xylene $>$ *m*-xylene $>$ *p*-xylene) yields insight into the regioselectivity of metal binding. In agreement with DFT calculations, the experimental results suggest that the most stable geometry is one that places the methyl groups as close to the Mn center as possible without situating them on carbon atoms directly bonded to the metal.

Similar to the observed trend in the stability of the η^2 interaction from benzene to the xylenes, the strength of the metal–(η^6 -arene) bond was previously found to increase with increasing methyl substitution [$\text{C}_6\text{H}_6 < \text{C}_6\text{H}_5\text{CH}_3 < \text{C}_6\text{H}_4(\text{CH}_3)_2 < \text{C}_6\text{H}_3(\text{CH}_3)_3 < \text{C}_6\text{H}_2(\text{CH}_3)_4 < \text{C}_6\text{H}(\text{CH}_3)_5 < \text{C}_6(\text{CH}_3)_6$].¹⁵ The greater stability of the η^6 interaction for the more substituted arenes is likely due to the increase in the σ donor ability of the aromatic ligand with increasing methyl substitution. Similar electronic considerations also apply in the case of η^2 binding to relatively electron-poor metal centers. However, a closer approach of the CH_3 substituents to the metal center in η^2 relative to η^6 binding results in an unfavorable steric interaction and hence a weaker bond between Mn and mesitylene than might otherwise be expected.

Acknowledgment. This work was supported by the National Priorities Research Program (NPRP, Grant 8-6-7-1) and the Undergraduate Research Education Program (UREP 5-1-3) administered by the Qatar National Research Fund (QNRF).

OM801185T

(14) At the B3LYP/6-31G* level of theory, the $\text{CpMn(CO)}_2\text{-(CyH)}$ binding energy was calculated to be 35.6 kJ/mol, similar to the previously determined value of 31.6 kJ/mol using a slightly different basis set (see ref 8a). Both estimates are lower than the calculated value of 38.4 kJ/mol for the strength of the $\text{CpMn(CO)}_2\text{-(mesitylene)}$ bond.

(15) (a) Muetterties, E. L.; Sievert, A. C. *Inorg. Chem.* **1981**, 20, 489. (b) Mahaffy, C. A. L.; Pauson, P. L. *J. Chem. Res. Miniprint* **1979**, 1746. (c) Klabunde, K. J.; Anderson, B. B.; Bader, M.; Radonovich, L. J. *J. Am. Chem. Soc.* **1978**, 100, 1313. (d) Halpern, J.; Riley, D. P.; Chan, A. S. C.; Pluth, J. J. *J. Am. Chem. Soc.* **1977**, 99, 8055.